The EXPLORE/OC Survey: Strategies and Selected First Results

Kaspar von Braun, Brian L. Lee, Sara Seager, H. K. C. Yee, Gabriela Mallén-Ornelas, and Michael D. Gladders

1. Abstract/Introduction

EXPLORE/OC is a photometric monitoring survey of southern Open Clusters with the aim of finding transiting planets around cluster-member main-sequence stars. The choice of observing open clusters was made to take advantage of the known (or calculable) astrophysical parameters common to all cluster member stars, such as age, distance, metallicity, and foreground reddening. The knowledge of these parameters enables us to a) target specific stellar radii by adjusting exposure times, and b) readily correlate the presence or absence of planets around member stars with the astrophysical properties of the target cluster. Furthermore, the study of the open cluster environment provides a complement to our ongoing deep monitoring surveys of rich Galactic fields (the EXPLORE Project).

In this presentation, we illustrate some of the advantages and challenges involved with transit finding and open cluster work, describe our observing and data-analysis strategies, and show some selected preliminary results of our study using the Carnegie Institution's Swope 1m Telescope at **Las Campanas Observatory** in Chile.

2. Target Selection Strategy

Target selection is difficult due to very limited availability of data on Galactic open clusters. To maximize the number of stars observed for long periods of time at high relative photometric precision, we base our target selection on:

- observability of the cluster (P_{vis}; see **Fig. 1**)
- distance to the cluster, which determines what relative photometric precision we attain for a given telescope, exposure time, and foreground reddening (see **Fig. 2, 3**)
- number of stars we can monitor at high relative photometric precision, cluster-members or not (see **Fig. 4**)

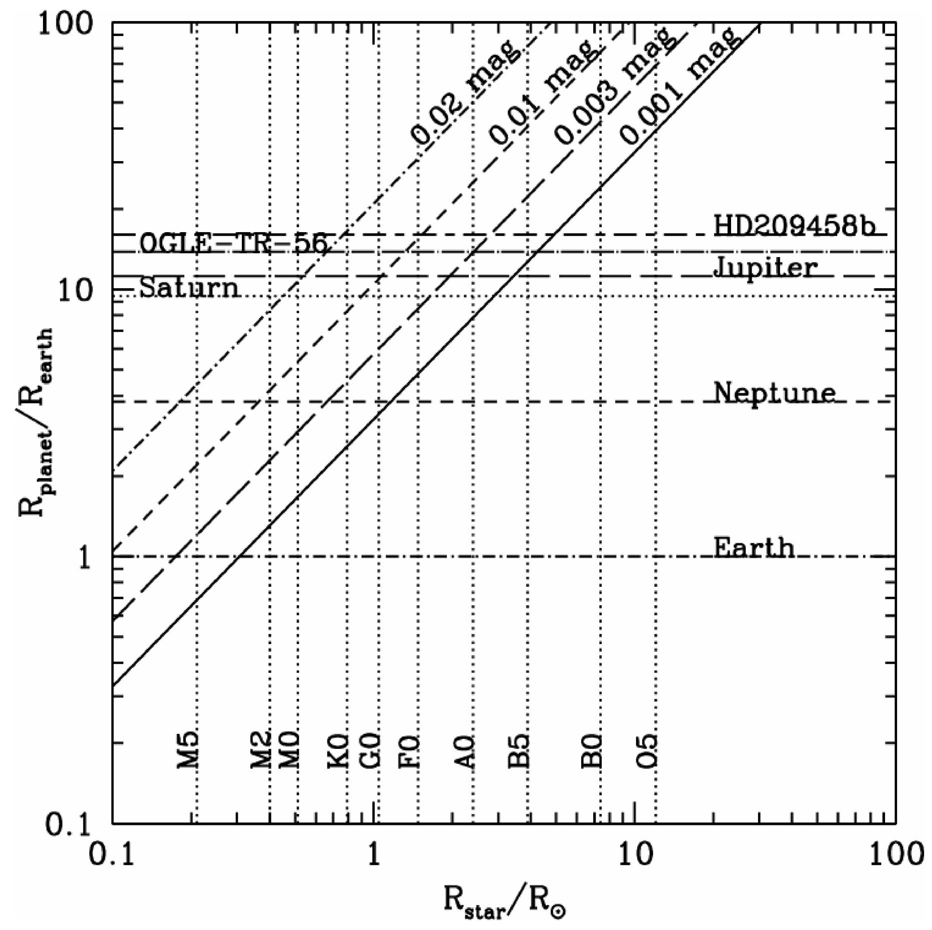

Fig 2: Relative photometric precision necessary to detect transiting planets with different radii as a function of MK spectral type and stellar size. For a given relative photometric precision, indicated by the diagonal lines, any combination between stellar and planetary radii located to the top-left of the diagonal line will be detectable. For instance, a relative photometric precision will enable detection of Jupiter-sized planets around stars of spectral type G0 or later. We typically reach relative photometric precision of 1% or better for stars with 14.5 < I < 17.0 (see **Fig. 3**)

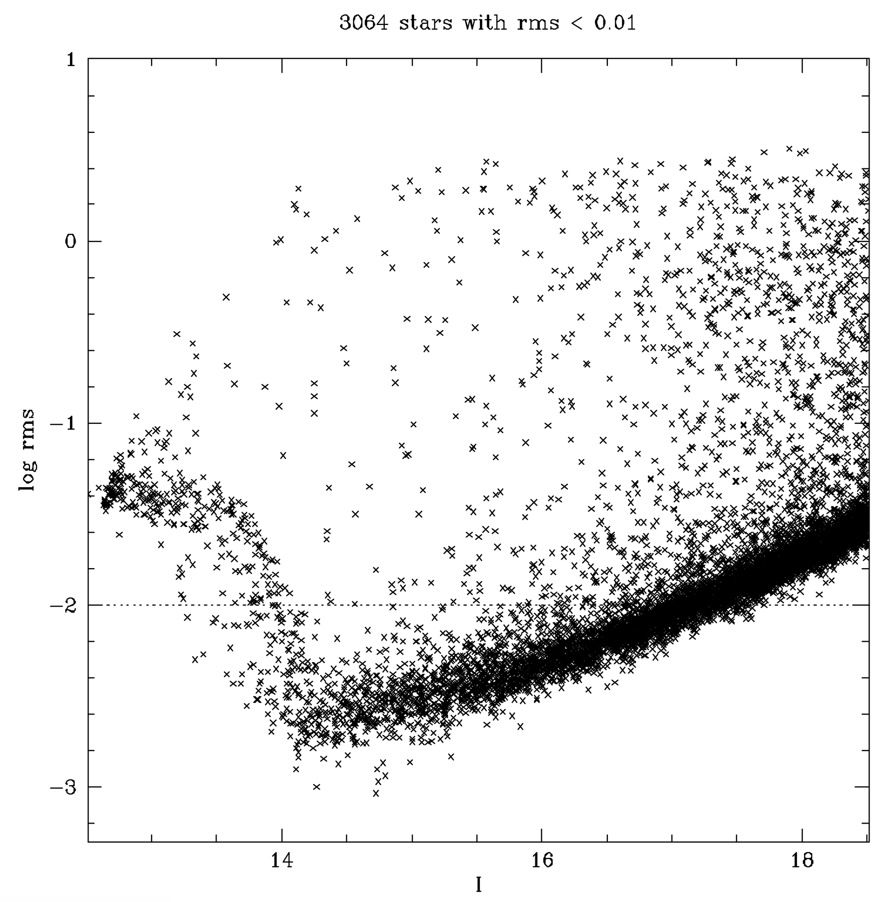

Fig 3: Photometric precision of night 1 of our monitoring run of **NGC 2660**. Of the roughly 21000 stars shown in this diagram, slightly more than 3000 have photometry of precision 1% or better. This rms is measured as the scatter around the mean magnitude of the star under investigation. The 1% photometry stars cover a magnitude range of slightly above 2.5 mags (14.5 < I < 17.0). By adjusting the exposure time, one can therefore target OC member stars of a range of certain spectral types (cf **Fig. 2**) to maximize the likelihood of detecting a transit (taking into account distance to the cluster and foreground reddening).

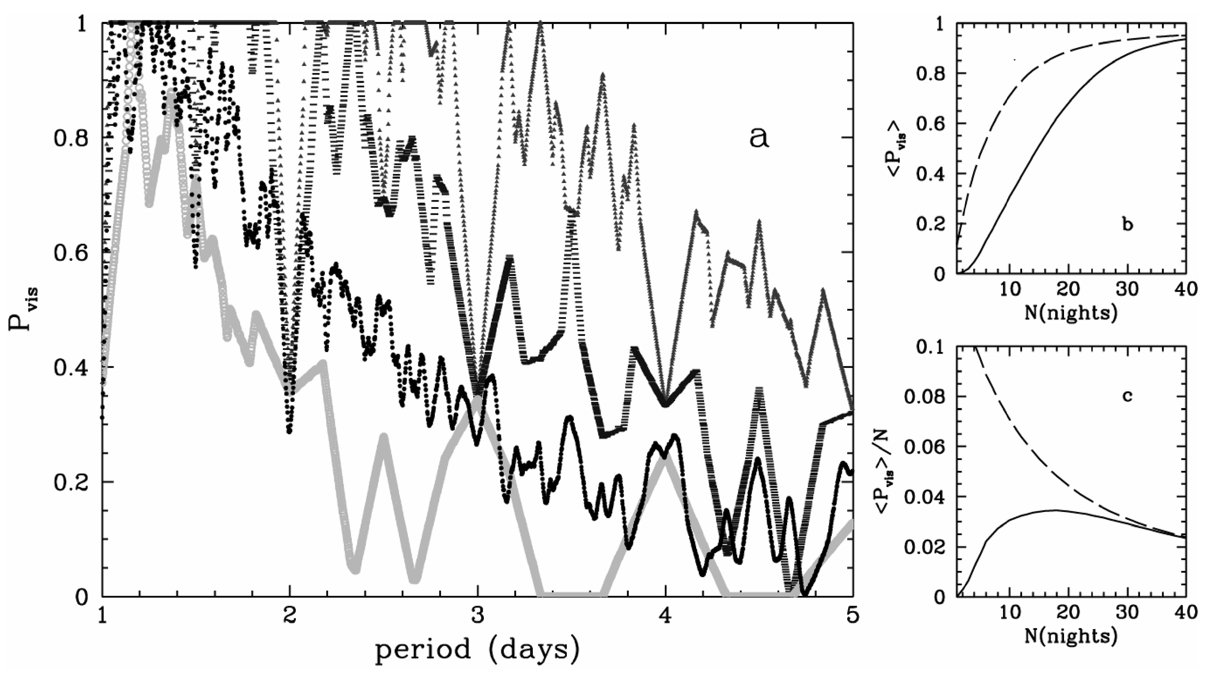

Fig. 1: Probability P_{vis} of detecting existing transiting planets with different orbital periods. P_{vis} is calculated with the requirement that two transits must be observed.

Panel a: P_{vis} of detecting 2 transits of an existing transiting planet with 1-5 days periods after 21 (**red triangles**), 14 (**blue bars**) and 7 (**green circles**) consecutive, uninterrupted nights of observing (10.8 hours per night). The difficulty of detecting some phase angles is shown by the dips in the curves (for instance, orbital periods of an integer number of days may always feature their transits during the day and are therefore statistically harder to detect). All phases are considered for each period. The **black triangles** curve shows the real P_{vis} for our monitoring study of **NGC 2660** (19 nights of 7-8 hours per night, with interruptions due to weather and telescope scheduling; see **Fig. 7**).

Panel b: The mean $\langle P_{vis} \rangle$ as a function of number of consecutive nights in an observing run (10.8 hour nights). The solid line is for the requirement to detect two transits and the dashed line for one transit. This figure indicates how much higher the likelihood of finding existing transits becomes with an increasing number of nights in an observing run.

Panel c: The efficiency of $\langle P_{vis} \rangle$ per night. For the two transits requirement (solid line) and 10.8 hour long nights, an observing run of 21 nights is most efficient. For the single transit requirement, the efficiency decreases monotonically with the number of nights since additional nights will add less and less probability of detecting "new" transits.

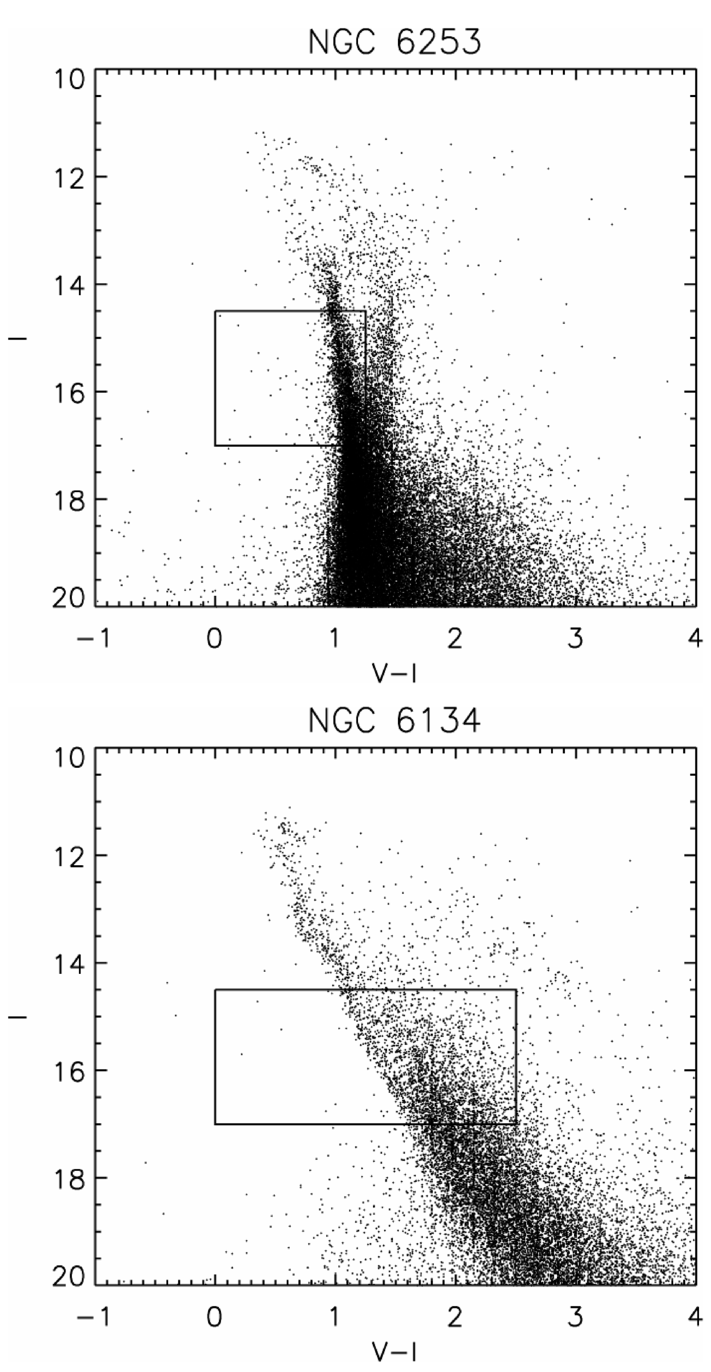

Fig 4: This Figure illustrates the process of our target selection, based on our own test data (calibrated based on a single standard field). Both of these two clusters were considered prospective targets for a June 2004 observing run. Since we know we can achieve 1% relative photometry for stars with 14.5 < I < 17.0 (cf **Fig. 3**), we count the number of stars in the boxes on the two CMDs. Note that we exclude the evolved red background sequence from consideration in the top panel since the stellar radii of evolved stars are too large for transit detection. Since the box in the CMD of **NGC 6253** contains more stars than (3400) the one in the CMD of **NGC 6134** (2600), we chose **NGC 6253** as the observing target.

3. Observing Strategy

Our observing strategy involves some of the following points:

- observe the target cluster as long as possible during a night, for ~20 nights without switching targets (see **Fig. 1**)
- observe in the I band to be able to discriminate between real transits and false positives (**Fig. 5**)
- high-cadence observing to temporally resolve the individual contact points of a transit (**Fig. 6**)

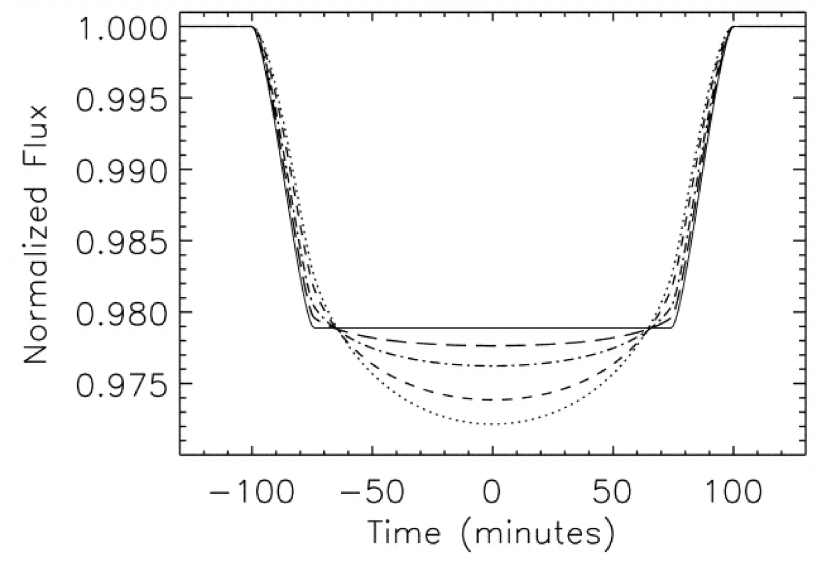

Fig 5: Solar limb darkening dependence of a central (i = 90) planet transit light curve. The planet has R = 1.4 RJ (approximately that of HD 209458b), and the star has R = Rsun. The solid curve shows a transit light curve with limb darkening neglected. The other curves, from top to bottom (at time = 0), show central transit light curves with solar limb darkening for wavelengths 3, 0.8, 0.55 and 0.45 microns. Note that the redder bands exhibit a shallower eclipse (stellar size appears larger since one observes the redder layers of outer atmosphere of the star), but have a more boxy appearance which distinguishes them from signals due to, e.g., grazing eclipsing binaries.

Figure from Mallén-Ornelas et al. 2003, ApJ, 582, 1123

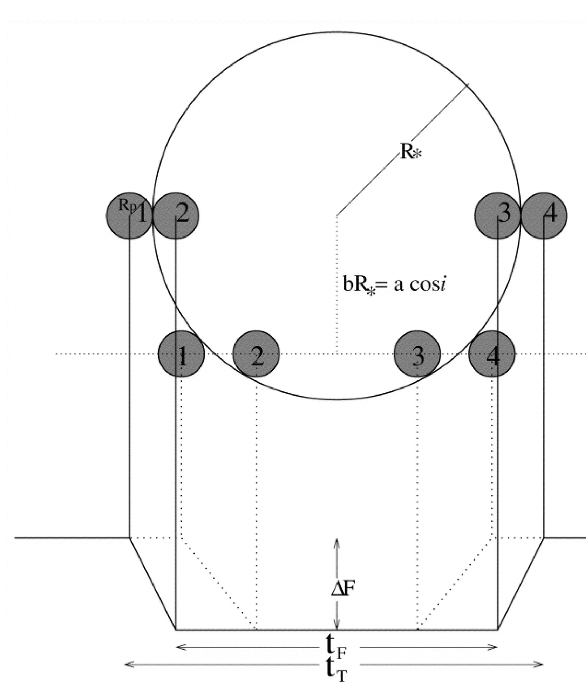

Fig 6: Schematic representation of the elements of a typical transit light curve. By temporally resolving the observables period, transit depth (ΔF), duration of totality (t_T), and total transit duration (t_F), one may calculate the system parameters planetary radius, inclination angle, orbital radius, and stellar density. The applicability of this "unique solution" justifies our high-cadence observing during monitoring.

Figure from Seager & Mallén-Ornelas 2003, ApJ, 585, 1038

4. Selected Results

We present some of our preliminary results on:

- typical light curves we obtain using our data reduction pipeline (**Fig. 7**)
- contamination of the cluster fields by Galactic field stars (**Fig. 8, 9**)

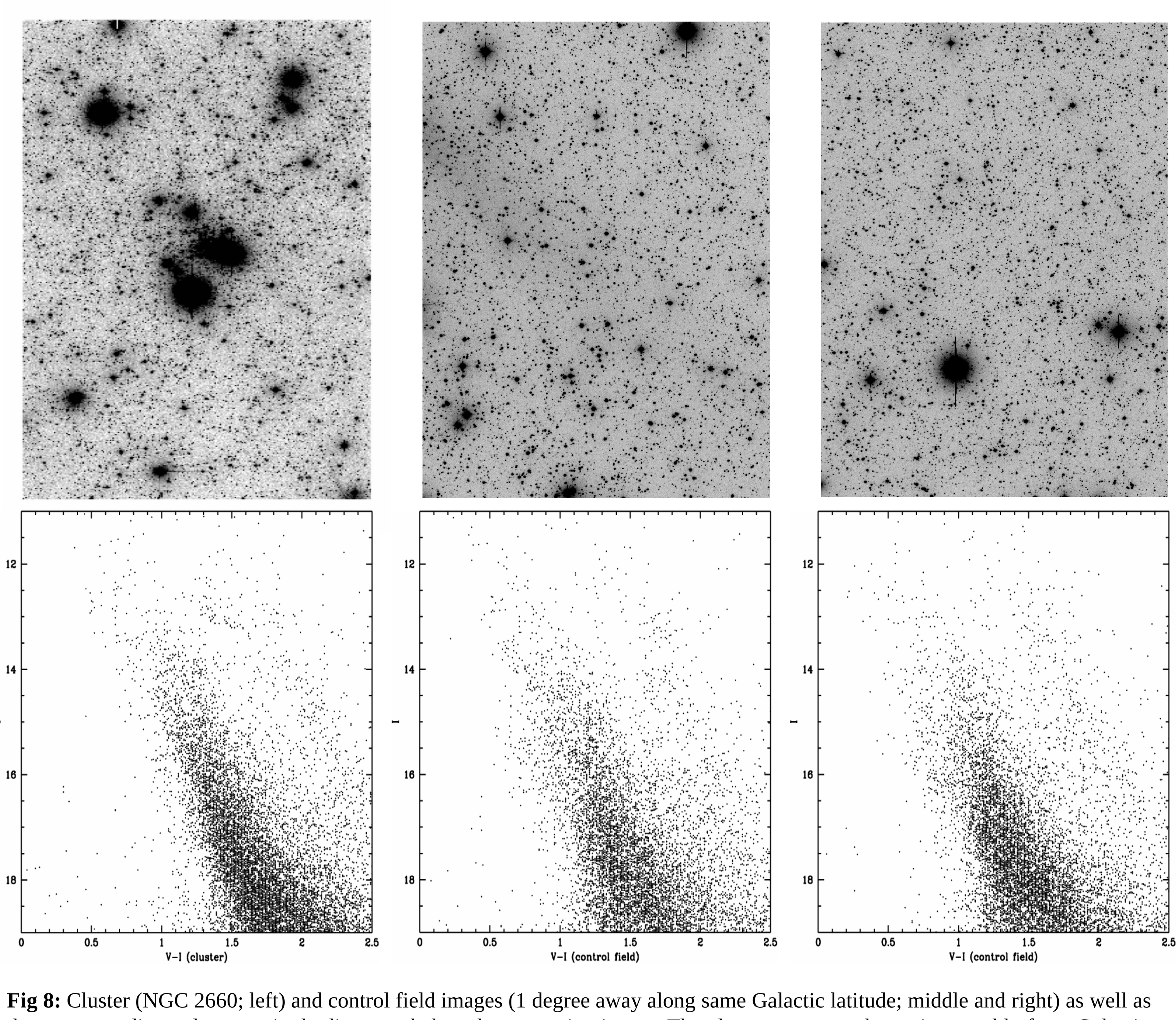

Fig 8: Cluster (NGC 2660; left) and control field images (1 degree away along same Galactic latitude; middle and right) as well as the corresponding color-magnitude diagrams below the respective image. The cluster stars are almost inseparable from Galactic field stars. Contamination is a serious issue in open cluster research (see **Fig. 9**).

For additional information, you may visit:

http://www.ciw.edu/seager/EXPLORE/open_clusters_survey.htm

(EXPLORE/OC web site)

Kaspar von Braun: +1 (202) 478-8859; kaspar@dtm.ciw.edu

Fig 7: Examples of real-time (unphased) light curves from our monitoring run of **NGC 2660**. Every panel represents data taken during one night, starting on the bottom left with night 1. Night 2's data are directly above it, night 3 above that and so on. We did not obtain any data during nights 13-15. Note that the magnitude scale is different for every panel shown. All these light curves were obtained in quasi-real-time at the telescope to implement a dynamic observing strategy to maximize observing / P_{vis} efficiency for a given number of nights.

Panels **a – d** show a number of variable stars we typically detect in the open cluster fields (from left to right: contact binary, detached binary, RR Lyrae pulsator, delta Scuti irregular pulsator).

Panels **e – g** display the kind of low-amplitude signal that we are looking for in the search for planetary transits. They are, however, most likely caused by non-planetary phenomena, such as a stellar-sized companion (panel e) or grazing binaries (panels f & g). Our spectral-type analysis indicates that panel e is an early G star, panel f is a late A star, and panel g is an early to mid F star.

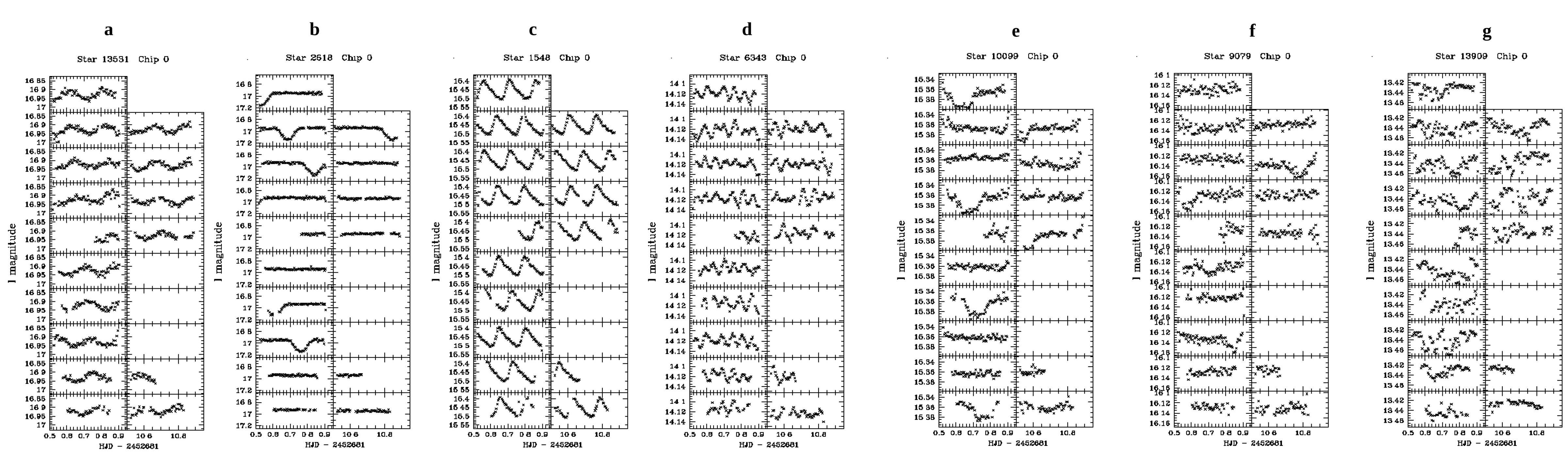

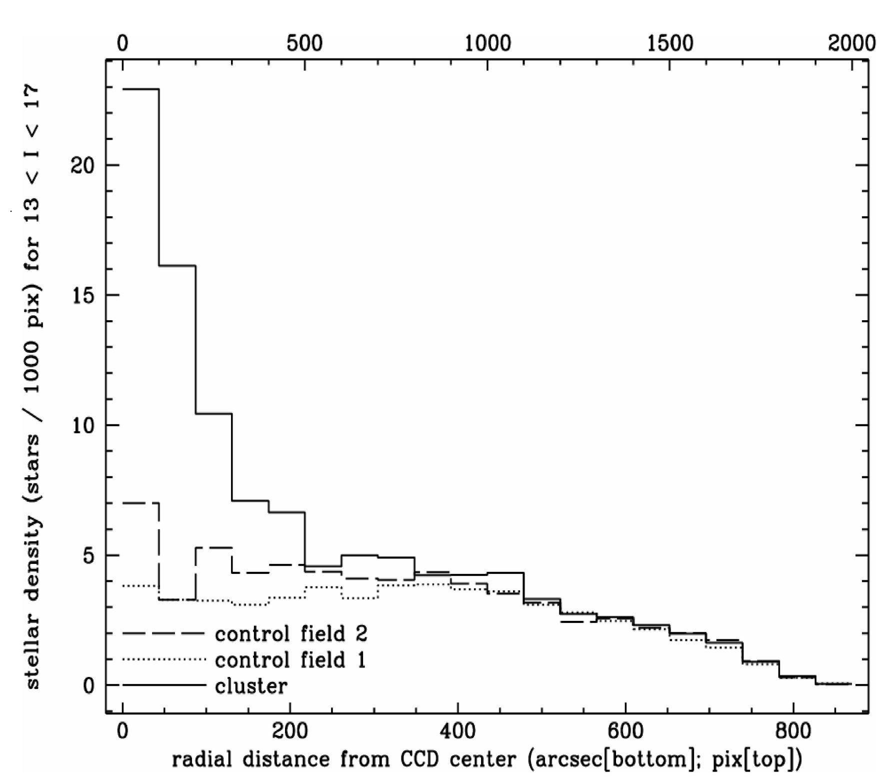

Fig 9: This figure compares the stellar density (measured in stars per 1000 pixel for 13 < I < 17) as a function of radial distance from the cluster center. The cluster field is indicated by the solid line, the control fields by the dotted and dashed lines. The drop-off in stellar density past 1000 pixel is a geometrical effect due to the rectangular shape of the CCD (see **Fig. 8**). The total number of stars under the curves is 3500 for the cluster field and 2800 average for the two control field, corresponding to a contamination of ~80% over the entire field and ~30% to a radial distance of 500 pix (~4 arcmin).